

LAND AND USE COVER CHANGE ASSESSMENT OF AN AGRICULTURAL AREA IN ROMANIA USING REMOTE SENSING AND CONSIDERING ENVIRONMENT CHANGE

*Prof. PhD LEVENTE DIMEN, Assoc.prof. PhD TUDOR BORȘAN
“1 Decembrie 1918” University of Alba Iulia, Romania
Prof. PhD BENJAMIN GATES, Edith Cowan University, Australia*

ABSTRACT: *The paper presents major aspects of the land use change. Changes in land coverage such as deforestation, agricultural expansion and urbanization have been identified to be not only a consequence of environmental change but also a significant cause driving further changes globally in response to the altering of biogeochemical cycles. Economic performance of Agriculture is therefore directly impacted by climatic conditions which invariably alter energy flows and consequently the performance, health and persistence of both crops and other land cover.*

This study intends to assess and compare the recent the land cover/land use within the small region of Crăciunelul de Jos, Romania using RS and GIS processing to provide localized insight regarding the environmental shifts and expansion of this region

Keywords: *Land use; agriculture; GIS; Remote sensing;*

Historically, land has been altered naturally over time and via human activities to take advantage of resources (farming, water and urbanization), however it is a growing understanding that land use changes are impacted on a global scale due to human activities influencing environments [Gries & Redlin, 2019]. The characteristics and patterns of land cover are essential factors underlying biophysical processes and key for developing models of the Earth's surface to understand the influence of anthropogenic activities [Bounoua et. al 2002; Herold et al 2008]. The appropriate management of resources, development strategies and conservation practices are dependent on the understanding of land cover information [Gómez, White, & Wulder, 2016].

This study intends to assess and compare the recent the land cover/land use within the small region of Crăciunelul de Jos, Romania using RS and GIS processing to provide localized insight regarding the environmental shifts and expansion of this region. Accuracy assessment will be carried out to indicate how well the RS imaging is

classified. The need for further investigation and monitoring of geospatial parameters will be identified by the comparison where necessary to encourage or maintain sustainable development goals. The analysis would prove to be of particular use to both business and government stakeholders for future land use planning and projects as Romania continues to grow and develop.

1. Methods

1.1. Area of study

Crăciunelul de Jos is a small village within the Alba county of Transylvania, located at 46.1715° N, 23.8361° E [Google Maps, 2020]. The assessment was limited to the land area within the Romanian communal boundary of Crăciunelul de Jos, covering approximately 25.25 km². The village itself falls within the Târnava Valley with elevations ranging between 225m and 396m above sea level and is positioned along the Târnava River, which was designated as a Site of Community Interest (SCI) area in

2013 by Natura 2000. Existing data for this SCI identifies the area as possessing a high-ranking input of Nitrogen pollution and no existing management plan (Natura 2000, 2019). The Târnava River forms from the confluence of the Târnava Mare and Târnava Mica rivers; and is one of the major tributaries of the Mureș River of up to 21% of the watershed [Bănăduc, 2005]. The basin of the Târnava Mare and Mica rivers houses the successful Târnava Vineyards run by the Jidvei Winery [Coros, Pop & Popa, 2019].

The climate of the locality is considered continental temperate and classified as Cfb under the Köppen-Geiger climate classification system. Average temperatures range from -0.9 and 19.3 degrees Celsius between summer and winter respectively and annual precipitation averages 572mm , with the majority occurring in summer [Climate-Data, 2020. The temporal focus of] the assessment will surround the month of April; the middle of Romania's spring period with average temperatures of 10.8°C and precipitation of 47mm . The map of the study area is shown in Figure 1.

General descriptions of various points of interest and landforms describing Crăciunelul de Jos are already compiled [Mărculeț I. & Mărculeț C. 2017], however not enough specific information regarding the distribution, coverage and environmental statistics exist in a compiled manner to conceptualize the area in a way which adds value to this land use assessment. Consequently, intuitive decisions and descriptions are made for the classification of land types of this assessment (table 1a).

1.2. Data Acquisition and processing

Multiband spectral images originating from the Sentinel-2B satellite were acquired via the United States Geological Survey (USGS) EarthExplorer portal; which redistributes Sentinel data products originating from the European Space Agency (ESA) Copernicus program. The Sentinel data was preprocessed by the ESA to Level-1C products and repackaged by USGS into tile-based bundles for distribution. The Sentinel-2B satellite uses a multispectral

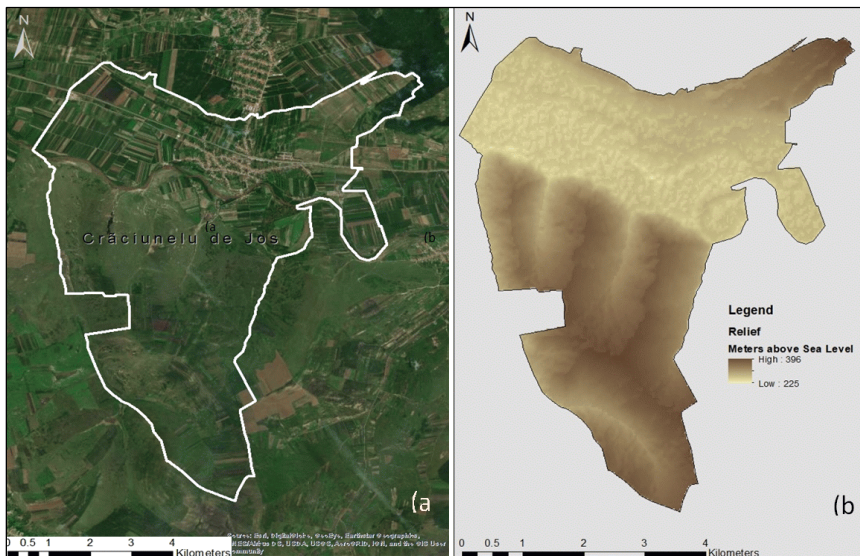


Fig.1. (a) Area of study; Crăciunelul de Jos within white boarder.
(b) Composite shaded relief map

instrument (MSI) to acquire 13 electromagnetic spectral bands ranging from 443nm to 2190nm wavelengths. The predominant bands of interest for this analysis were bands 2, 3, 4, 8 and 11 (490nm blue, 560nm green, 665nm red, 842 visible and near infrared/VNIR and 1610nm short range infrared/SWIR respectively), selected for their implementation in vegetation indices, detailed spatial resolution of 10m (20m for SWIR) and pre-processing level. The specific datasets used for temporal comparisons were selected to have the most comparable dates to minimize seasonality differences in land cover/usage, global positioning and weather variables. The selected datasets were 27th April 2016 and 23rd April 2020 for their date proximity and minimal cloud cover.

The Digital elevation model (DEM) was also acquired via the USGS EarthExplorer, however data used originated from the Space Shuttle Endeavor during the Space Shuttle Radar Topography Mission (SRTM), 11 February 2000. The SRTM developed topographical models with resolutions of 30m (1 arc-second) which have been widely accessible online since September 2014. It is worth noting that SRTM data has been edited to fill small voids, remove spikes and wells, delineate and flatten water bodies and define coastlines with larger areas of missing data being filled by the National Geospatial-Intelligence Agency (NGA) using other sources of elevation data in conjunction with interpolation algorithms.

All image processing during the analysis was achieved using ArcMap 10.7 software and implemented the projected coordinate system WGS 1984 UTM Zone 34N. Data from the acquired DEM and spectral images were geometrically extracted to the coordinates of the Crăciunelul de Jos regional boundary outlined by the Romania Regiuni Boundaries 2017 feature service provided by Esri via the ArcGIS online database.

1.3. Spatial Analysis

Analysis of the spectral images involved the calculation of several remote sensing (RS) indices, including Normalized Difference Vegetation Index (NDVI), Normalized Difference Moisture Index (NDMI), Bare Soil Index (BSI) and Normalized Difference Water Index (NDWI) using the raster calculator. Layer stacking and comparison of the different indices assist in the visual interpretation of the multispectral image, particularly changes in land coverage [HemaLatha, Varadarajan & Pandian, 2019]. The calculated Indexes return values on a scale between -1 and 1 which correlate with different surface conditions based on the reflectance of the associated bands.

NDVI is a significant vegetation index applied to a range of studies globally involving environment, climate change and land monitoring. The NDVI is highly related to vegetation content, typically utilized to quantify the photosynthetic capacity of vegetation [Rahman & Mesev, 2019). NDVI utilizes bands 8 and 4 to measure the reflectance ratio of red and near infrared wavelengths whereby greater reflectance corresponds to denser, healthier vegetation. NDVI is determined using the equation:

$$\frac{(Band\ 8 - Band\ 4)}{(Band\ 8 + Band\ 4)}$$

NDMI implements the normalized difference of the bands 8 and 11 (VNIR and SWIR) where the reflectance highly correlates to canopy water content (Jin & Sader, 2005). The NDMI was calculated using:

$$\frac{(Band\ 8 - Band\ 11)}{(Band\ 8 + Band\ 11)}$$

The BSI acts as an indicator to assist in the capture of bare soil and soil variations, combining the bands 11, 4 and 2 (SWIR, red and blue) whereby higher values indicate there is more bare soil. BSI was calculated as follows:

$$\frac{(Band\ 11 + Band\ 4) - (Band\ 8 + Band\ 2)}{(Band\ 11 + Band\ 4) + (Band\ 8 + Band\ 2)}$$

The NDWI uses bands 3 and 8 (green and VNIR) and is often used in conjunction with NDVI for mapping vegetation and surface waters [Jackson et al. 2004]. Greater reflectance is relative to greater water content. NDWI was calculated with the formula:

$$\frac{(Band\ 3 - Band\ 8)}{(Band\ 3 + Band\ 8)}$$

Manipulation of the DEM enhances the visualization of topography via the creation of contour, relief shading, aspect and incline layers using arcGIS toolsets. Topography has been shown to influence land usage suitability due to physical variables including elevation, hydrology, sunlight/shadowing and erosion [Elsheikh, 2013]. Creation of these layers add value to the analysis of land cover change by identifying correlations between topographical features in relation to land cover extent using the layer stacking technique. Inherent errors are known to exist in DEMs and amplified when manipulated [Wechsler, Hyowon, & Li, 2019], as such this data is used qualitatively as opposed to a geospatial truth.

Land use classification followed the supervised classification method. This classification technique can be defined as the development of spectral signatures by the

user, implementing training sites representative of known land cover such as urban or forest, before software assigns each pixel in the image the class which its signature is most comparable to [Eastman, 2003]. For this analysis the spectral reflectance of the blue, green, red and VNIR bands were compiled into composite layers (RGBNIR colour composite) to provide the data for training classes. Training sites were selected from across the area of study and compiled into 7 different land cover classes which were saved as a signature file with classes defined as in table 1. Class determination utilized a combination of visible features from a true colour composite and the land cover indices previously determined.

Maximum likelihood classification (MLC) algorithm was selected for this classification as it is one of the most widely used. The MLC depends on the probability distribution of the feature classes as per the Bayes' theorem; with the algorithm determining the probability of each pixel belonging to those classes and then assigning the most likely as the resulting land cover [Richards, J. A. 2014]. This type of classification is largely controlled by the analyst and which pixels are selected to be representative of the classification, with satisfactory spectral signatures resulting in minimal confusion between classes [Gao & Liu, 2010].

MLC:

$$g_i(x) = \ln p(\omega_i) - \frac{1}{2} \ln |\Sigma_i| - \frac{1}{2} (x - m_i)^T \Sigma_i^{-1} (x - m_i)$$

Table 1. Land cover classes and respective user definitions for multispectral image classification

Class	User definition
Water	Areas where visible surface waters are present.
Fallow	Farmland without evident vegetation.
Agriculture	Farmland with evident vegetation growth.
Urban	Combination of roads, buildings and housing.
Grassland	Healthy grassland meadows with an NDVI greater than 0.5
Degraded Grassland	Visibly sparse grassland meadows with an NDVI below 0.5
Tree Canopy	Locations where tree density obscures other land cover.

Where:

i = class

x = n-dimensional data (where n is the number of bands)

$p(\omega_i)$ = probability that class ω_i occurs in the image and is assumed the same for all classes

$|\Sigma_i|$ = determinant of the covariance matrix of the data in class ω_i

Σ_i^{-1} = its inverse matrix

m_i = mean vector

1.4. Statistical Analysis

Determining the statistical accuracy of the classifications is vital for understanding quantitatively how well the classification model identifies pixels as the correct land cover class. For this study an error matrix, also known as confusion matrix [Eastman, 2003], was generated by selecting an equal number of known pixels (unrelated to the training groups) from each land cover type and comparing how many pixels were correctly or incorrectly identified. A total of 120 pixels were manually selected for each temporal map, ranging across the entire geographical extent. Known pixels were clearly identified using the Sentinel high resolution true colour images and comparison of the calculated indexes to ensure high levels of confidence. This is the best method available due to the lack of obtainable field data confirming coordinates and land cover for these temporal periods.

Based on the compiled error matrixes statistics can be calculated; for this study user accuracy, production accuracy and overall accuracy are calculated. Accuracy from the perspective of the map user (user accuracy) shows how often the map class is representative of the class on the ground, otherwise referred to as reliability and is calculated by dividing the total number of correctly identified sites by the number of sites classified. Accuracy from the perspective of the map maker (producer accuracy) represents how often real features

are appropriately represented on the map and calculated by dividing the number of correctly classified reference sites by the number of total reference sites. Overall accuracy represents the probability that points are correctly identified by the classification and compares the user and producer accuracies, calculated by total number of correct predictions divided by the total number of predictions.

Additionally, the Root Mean Square Error (RMSE) is calculated to determine the root square of the variance of the residuals, indicating the absolute fit of the model in meters. RMSE is known to be the most important measure for determining the accuracy of prediction fit within a model [Abdulrazak, 2018]. The RMS equation implemented is:

$$RMSE = \sqrt{\frac{\sum_{i=1}^N (O_i - S_i)^2}{N}}$$

Where: O_i = observed value

S_i = predicted value

N = number of samples.

2. Results

Figure 1b identifies the geographical relief of the study area with an elevation range of 171 meters between a 396 high and 225 meters low (above sea level). Three distinct ridgelines exist along the North North-East axis, forming valleys and drainage pathways to an expansive floodplane surrounding the Târnava River. The overall degree of incline throughout the region undulates between 0 and 4 degrees, however inclination angles climb sharply towards the ridgeline peaks on the southern side of the floodplain before flattening (fig. 2b). The undulations throughout the floodplain creates slopes facing all directions however Southern slopes are seen to cover the most amount of land area within the region compared to other directions. Flat ground (slope of 0) was mostly absent (fig. 2a).

The NDVI comparison identifies a clear shift in vegetation reflectance and coverage (figure 3); maximum and minimum NDVI values dropped by approximately 0.06 between 2016 and 2020 whilst the mean NDVI for the region dropped from 0.866 to

0.386.

The overall distribution of NDVI points (as per figure 4) shifted to indicate more pixels falling within a threshold 0.1-0.2, suggesting a larger area has minimal vegetative cover compared to 2016.

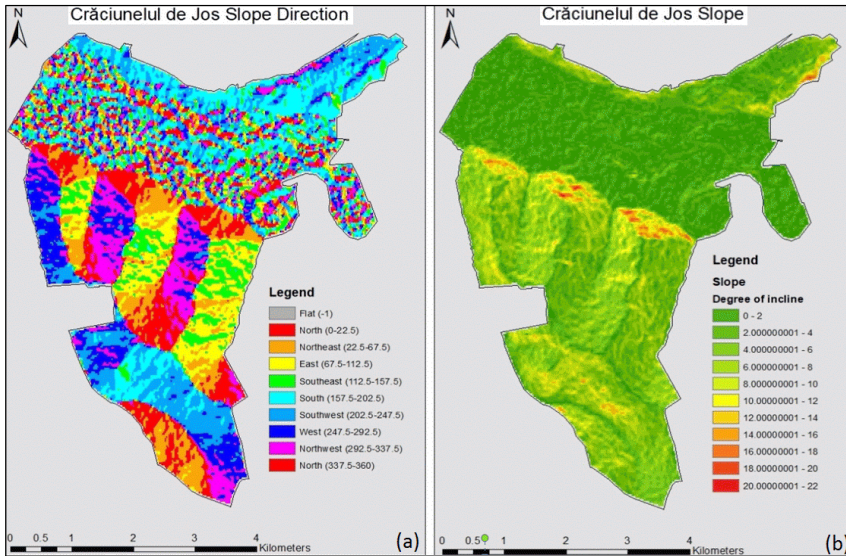


Fig. 2. (a) Colour coverage map representing slope direction.
(b) Colour map representing angle of slope

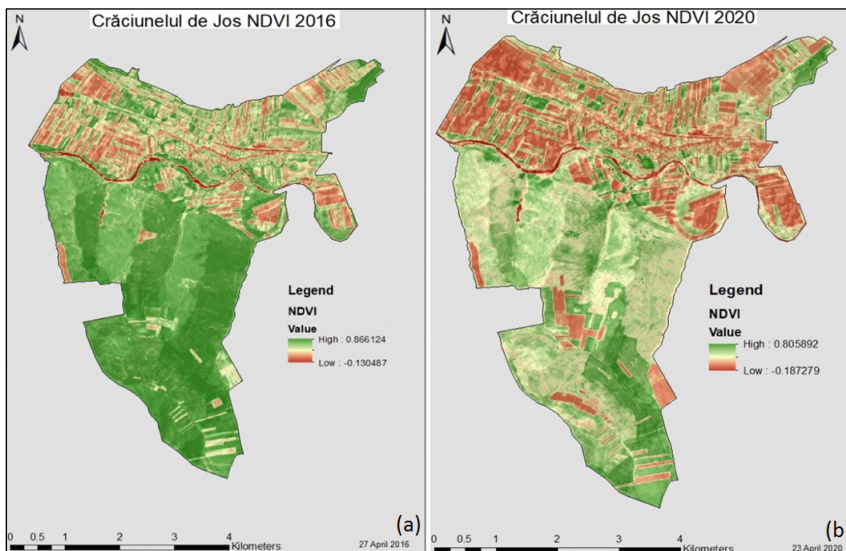


Fig. 3. (a) Normalised Difference Vegetation Index map 2016
(b) Normalised Difference Vegetation Index map 2020

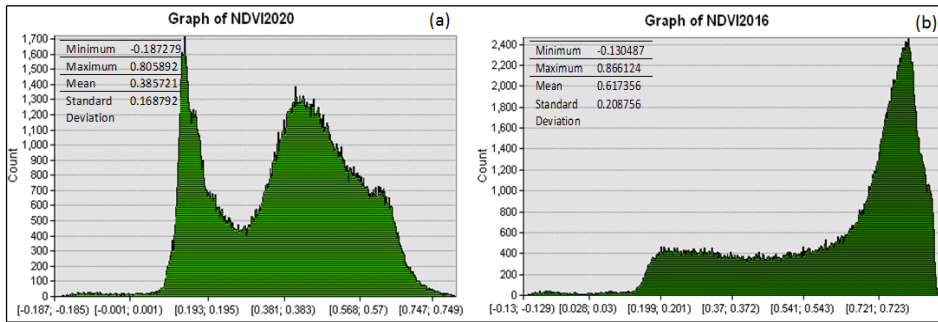


Fig. 4. (a) value frequency distribution of 2020 NDVI pixels
(b) value frequency distribution of 2016 NDVI pixels

NDMI identifies a similar trend showing the decrease of vegetation moisture content, correlating with the NDVI decrease in vegetation cover; with minimum and maximum values dropped by approximately 0.06 in 2020 compared to 2016 (figure 5). The mean NDMI also decreased from 0.24 to -0.02 in 2020, indicating lower average canopy cover and potentially higher water stress of remaining vegetation. The distribution of points identifies a majority of 2020 values falling between -0.2 and 0 which correlates with low canopy cover and high-water stress compared to the 0.6-0.8

distribution seen in 2016.

NDWI clearly identifies the Tarnava River and an unidentified small lake/seasonal tributary in both datasets (figure 7). NDWI product values suggest an overall increase in surface water content in 2020 compared to 2016 with maximum and minimum values increasing by approximately 0.04 and 0.07 respectively (figure 7).

Analysis of the data distribution (figure 8) confirms the overall increase and could be representative of improving water stress in contrast with the NDMI results.

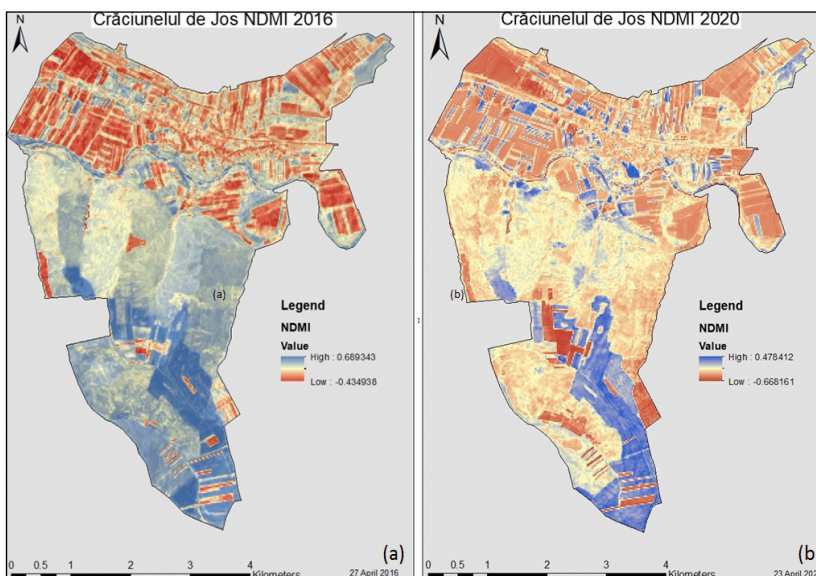


Fig. 5. (a) Normalised Difference Moisture Index map 2016
(b) Normalised Difference Moisture Index map 2020

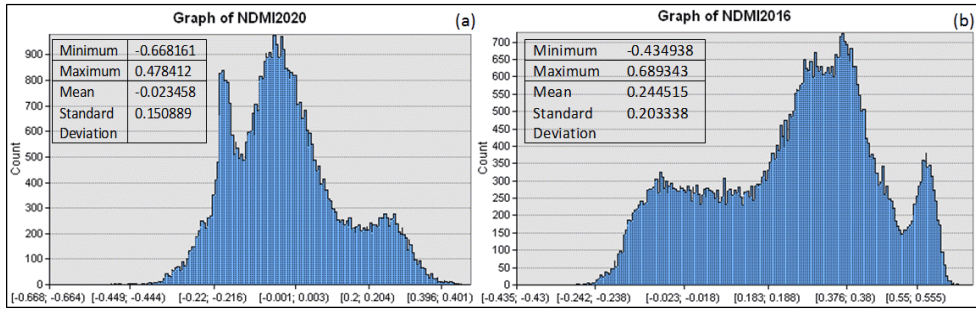


Fig. 6. (a) value frequency distribution of 2020 NDMI pixels
(b) value frequency distribution of 2016 NDMI pixels

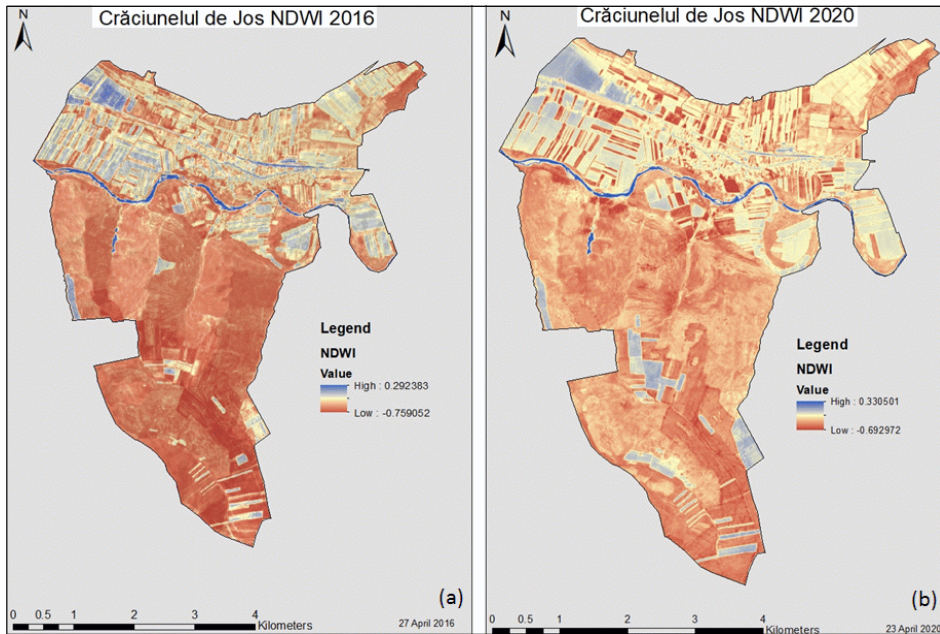


Fig. 7. (a) Normalised Difference Water Index map 2016
(b) Normalised Difference Water Index map 2020

Comparing BSI for the 2020 and 2016 data sees the maximum bareness increase by approximately 0.06 whilst minimum bareness increased by 0.18, indicating that bare soil coverage has increased in all areas (figure 9). A clear positive shift in the data distribution is observed between the years, increasing mean BSI by ~ 0.23 (figure 10).

The land use/land cover map for 2016 (figure 11a) is dominated by Grassland with 9235.6 m² coverage. This is followed by Urban (5071.9 m²), Agriculture (4474.6 m²) and Fallow (4164.8 m²).

Smaller areas of Tree Canopy exist (2105.9 m²) and even less water (198.1 m²), however no Degraded Grassland was identified (table 2).

The land use/land cover map for 2020 (figure 11b) was notably different; Grassland, Urban and Agriculture coverage decreased by 9.63%, 5.79% and 1.74% respectively. Water and Fallow increased marginally (0.24% and 6.13%), however Degraded Grassland was now detectable, covering 19.13% (table 2). No Tree canopy was detected in this classification.

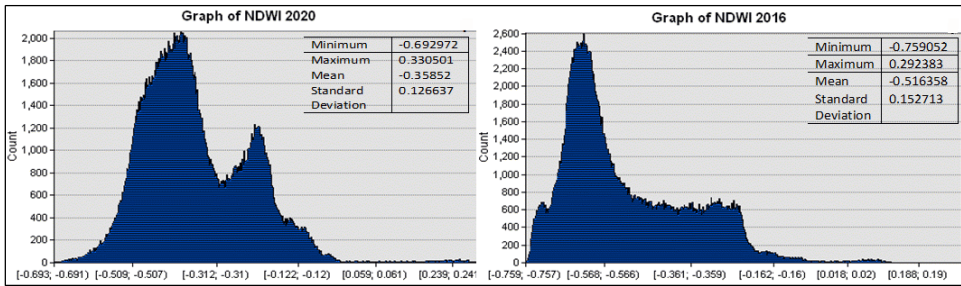


Fig. 8. (a) value frequency distribution of 2020 NDWI pixels (b) value frequency distribution of 2016 NDWI pixels

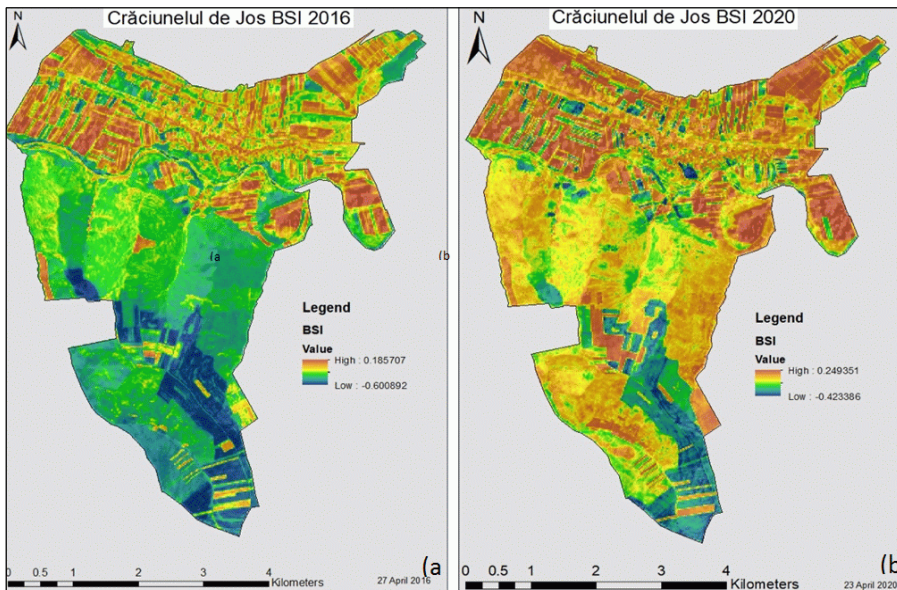


Fig. 9. (a) Bare Soil Index map 2016 (b) Bare Soil Index map 2020

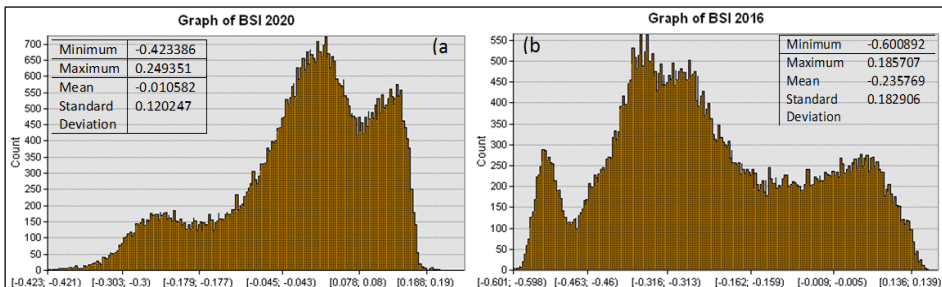


Fig. 10. (a) value frequency distribution of 2020 BSI pixels (b) value frequency distribution of 2016 BSI pixels

Table 2. Area of Land use/land cover type for April 2016 and 2020, calculating change

Land cover	2016	2016	2020	2020		
Class	Area (m ²)	Coverage %	Area (m ²)	Coverage %	Land coverage change m ²	Land coverage change %
Water	198.1	0.784526	258.3	1.022934	60.2	0.238407
Fallow	4164.8	16.49367	5712.9	22.62454	1548.1	6.130871
Grassland	9235.6	36.57533	6802.9	26.94122	-2432.7	-9.63411
Degraded Grassland	0	0	4832.4	19.13754	4832.4	19.13754
Tree Canopy	2105.9	8.339901	0	0	-2105.9	-8.3399
Urban	5071.9	20.08602	3610.3	14.29771	-1461.6	-5.78831
Agriculture	4474.6	17.72056	4034.1	15.97606	-440.5	-1.74449
Total	25250.9	100	25250.9	100		

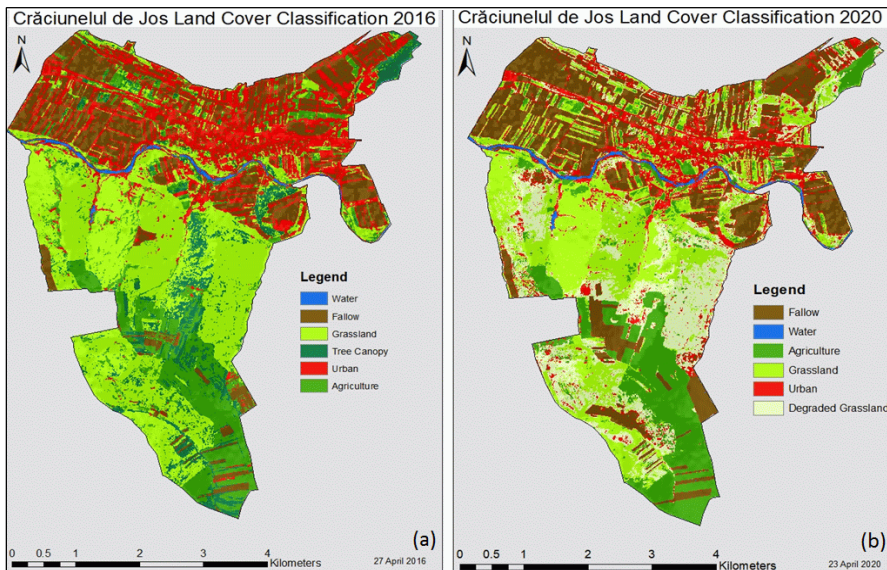


Fig. 11. (a) Land use/land cover classification map 2016.
 (b) Land use/ land cover classification map 2020

Classification accuracies for the generated models revealed that whilst overall accuracy was similar between the datasets (81.8% and 83.5%) relative user and producer accuracies were more variable between each land cover class (tables 3 & 4). The calculated RMSE returned comparable values between the two classifications (4.18m and 4.16m), which were lower than the 10m spectral resolution of the map, thus indicating good overall fit.

3. Discussion

All spectral indices observe the similar decreases in healthy vegetative cover and increased extent of bare soils, other recent studies indicate that the correlation between decreased moisture content (as visualized in figure 5) and other hydrological factors such as precipitation and temperature are often causal for such changes [Yang et al. 2019].

Table 3. Accuracy assessment for land cover classification model 2016

Classes 2016	Water	Fallow	Grassland	Tree Canopy	Urban	Agriculture	Total
<i>Water</i>	14	0	0	0	0	0	14
<i>Fallow</i>	2	18	0	0	2	0	22
<i>Grassland</i>	0	0	17	1	0	3	21
<i>Tree Canopy</i>	0	0	2	16	0	3	21
<i>Urban</i>	4	2	0	0	18	0	24
<i>Agriculture</i>	0	0	1	3	0	14	18
Total	20	20	20	20	20	20	
Producer Accuracy %	70.0	90.0	85.0	80.0	90.0	70.0	
User Accuracy %	100	81.8	80.9	76.2	75.0	77.8	
Overall Accuracy %	81.8						
RMSE (meters)	4.18						

Table 4. Accuracy assessment for land cover classification model 2020

Classes 2020	Fallow	Water	Agriculture	Grassland	Urban	Degraded Grassland	Total
<i>Fallow Agriculture</i>	15	0	0	0	0	0	15
<i>Water</i>	0	19	0	0	0	0	19
<i>Agriculture</i>	0	1	15	3	0	0	19
<i>Grassland</i>	0	0	5	16	0	2	23
<i>Urban</i>	5	0	0	0	20	4	29
<i>Degraded Grassland</i>	0	0	0	1	0	14	15
Total	20	20	20	20	20	20	
Producer Accuracy %	75.0	95.0	75.0	80.0	100	70.0	
User Accuracy %	100	100	78.9	69.5	68.9	93.3	
Overall Accuracy %	83.5						
RMSE (meters)	4.16						

Although no data regarding temporal specific precipitation and temperature were found for this region; broader climate changes for Romania identify overall decreased precipitation and increased temperatures, particularly in the past decade [World Bank Group, 2020], which are likely large factors influencing decreased land coverage and health of observed grasslands and tree canopy. Land identified as Agriculture show more consistent NDMI values between the temporal comparison compared to other types of vegetation, however this is possibly a result from ongoing shifts towards the need for irrigation and supportive farming practices to maintain

crop productivity. Further investigation towards specific farming practices is necessary to evaluate the sustainability of such methods due to the degradation of surrounding land cover.

The notable increase in overall NDWI could potentially be related to the overall increased area of bare soils due to the spectral reflectance of band 3 not being evaluated in the BSI. Consequently, soil mineralogy may be interfering with the NDWI due to shorter wavelengths between 400 μm and 1000 μm (inclusive of band 3) increasing reflectance for soils high in iron oxides [Huete, 2004]. Alternatively, it is speculated that poor soil drainage and recent

precipitation events in the 2020 dataset may be the cause for these higher average values and result in a disparate comparison within the scope of this study. Various areas of Fallow land depicted higher NDWI values for both the 2016 and 2020 maps and could be representative of saturated soils or influenced surface minerology due to farming practices including irrigation and fertilization. Future Analysis of soil profiles and characteristics within the region will assist in the interpretation of the variable NDWI and provide insight to soil suitability and degradation land cover classes.

The minor decrease in Agriculture coverage identified in this study (table 2) can be largely attributed to the increase in Fallow land and potential shift in farming practices reflective of environmental changes. Without exact knowledge of the crops and harvest times it is useful to combine Fallow and Agriculture classes to better represent the total land used for all agricultural practices. Thus, the total agricultural cover change can be considered a relatively small increase of 4.39% over 4 years. Agroforestry practices such as increasing tree coverage are shown to increase carbon biomass sequestration on agricultural lands, contributing to climate change mitigation [Zomer et al., 2016]. However, the complete removal of detectable Tree Canopy by 2020, likely due to expansions of nearby crop fields, identifies a total land cover area decrease of 8.34% suggesting the expansions to date have been inefficient and potentially unsustainable as a result. Studies of Romanian land determine that pursuit of sustainable development of agriculture is best achieved following organic farming practices, aiming to balance productivity with conservation [Aurelian, Paschia & Coman, 2019]. This tactic includes the use of perennial crops, increasing crop diversity and tree coverage to protect soil degradation whilst maintaining surrounding natural landforms and cover to protect and promote ecosystem services. Current land cover change suggests these

strategies may not be implemented effectively in this region, reinforcing the need for in-depth assessment of localized agricultural practices to identify improvements for achieving sustainable development.

The combined effect of vegetative degradation, potential anthropogenic practices and climate shifts are likely to increase future rates of soil erosion, runoff and costs for land management. Not only has previous research identified that erosion and sediment yield are influenced by the changing order of precipitation events, such as extended periods of drying before rainfall, but also the mitigation of such surface flows regardless of soil type is evident in vegetated areas [Williams, et al. 2019; Le, et al. 2020]. The surface flow patterns of Crăciunelul de Jos are easily visualized in the relief and slope direction maps (figure 1b and 2a), whereby the majority of surface flow will eventualize in the floodplains and Tarnava River. Increased erosion and runoff are likely to result in increased eutrophication locally and at other environments downstream, particularly due to the associated agricultural land cover in the floodplains themselves. Although floodplain farming practices can take advantage of greater water availability, increased degradation and climate change factors require a proactive approach to water quality monitoring and minimizing local contributions to the catchment. Rehabilitation of vegetative cover will likely improve potential future outlooks on erosion and surface flow, minimizing impacts on agricultural land and the Tarnava River.

The decrease in classified Urban coverage appears to be caused by classification error between the models. Visual inspection of both maps compared to the true colour image reveals that the 2016 dataset appears to classify Urban more extensively compared to 2020, however both models clearly classify many pixels as Urban when they should actually be Grassland or Fallow. Because of this disparity not clearly

reflected in the accuracy assessment, the Urban class coverage is unreliable for comparison. This may suggest other substantial errors not as easily recognizable in the classification models and future classifications would benefit from larger samples of known pixels being used as a reference when constructing the error matrix for statistical analysis. Consequently, all classes and the RMSE may be more variable than initially indicated in this study and land cover classifications should continue to be developed.

4. Conclusions

Use of remotely sensed data have allowed the visualization, classification and quantification of land use/land cover change, however lack of known land cover used may have introduced excessive bias and results should therefore be used qualitatively to depict overall patterns only.

Although Romania aims for sustainable development by 2030, it is identified that the region of Crăciunelul de Jos requires reeva-

luation surrounding climate and land use practices to approach this goal. This study has identified an extensive shift in vegetation cover and health in recent years.

Climate changes are likely to play a large role in vegetative degradation, however unsustainable agricultural practices and expansion will inevitably accelerate this process. It is suggested that soil analysis takes place to identify current soil characteristics for ongoing monitoring and suitability of production. Education and funding for sustainable developments could create project opportunities surrounding rehabilitation, analysis and increased productivity in the future.

The connectedness of this region with other parts of the county via the topography and Tarnava River make it particularly important for water and soil quality monitoring as local degradation related to land use could alter streamflow and impact communities and production downstream. Future studies are needed to accurately quantify and separate the effect of climate, topography, soil and vegetation influences based on the features and changes identified.

References

1. Aurelian, I. C.; Paschia, L., & Coman, M. D. (2019). *Romanian Agriculture and Sustainable Development*. 11th LUMEN International Scientific Conference Communicative Action & Transdisciplinarity in the Ethical Society. Targoviste, Romania. 156-169. DOI: 10.18662/lumproc.108.
2. Bănăduc, A. (2005). *Study regarding Târnava Mare and Târnava Mică rivers (Transylvania, Romania)*, Stonefly (Insecta. Plecoptera) larvae communities. *Transylvanian Review of Systematical and Ecological Research*. 2. 75-84 .
3. Bounoua, L.; DeFries, R.; Collatz, G.J.; Sellers, P.; Khan, H. (2002) Effects of land cover conversion on surface climate. *Climatic Change*, 52, 29–64. DOI: <https://doi.org/10.1023/A:1013051420309>.
4. Burkepile, D. E., & Hay, M. E. (2008). *Encyclopedia of ecology, five-volume set*. In *Coral reefs* (pp. 784–796). essay, Elsevier B.V. <https://doi.org/10.1016/B978-008045405-4.00323-2>.
5. Castillo, C. P.; Kavalov, B.; Diogo, V.; Jacobs, C.; Batista, F. E. S.; Baranzelli C., & Lavalle C. (2018). *Trends in the EU Agricultural Land Within 2015-2030*. JRC113717. European Commission 2018. <https://ec.europa.eu/jrc/en/publication/ur-scientific-and-technical-research-reports/rends-eu-agricultural-land-within-2015-2030>

6. Climate-Data (n.d.). *Crăciunelu de Jos Climate (Romania)*. Retrieved May 30, 2020, from <https://en.climate-data.org/europe/romania/alba/craciunelu-de-jos-146942/>
7. Cros, M. M., Pop, A. M., & Popa, A. I. (2019). *Vineyards and wineries in Aba county, Rmania, towards sustainable business development*. Sustainability (Switzerland), 11(15). <https://doi.org/10.3390/su11154036>.
8. Departmentul Pentru Dezvoltare Durabila/Department of Sustainable Development (2015). *Romania's Sustainable Development Strategy*. <http://dezvoltaredurabila.gov.ro/web/about/>
9. Eastman, J.R. (2003) *Guide to GIS and Image Processing 14*, 239-247. Clark University Manual, USA, Worcester, MA. Retrieved from: <https://www.mtholyoke.edu/courses/tmillet/course/geog307/files/Kilimanjaro%20Manual.pdf>
10. Elsheikh, R., Mohamed Shariff, A. R. B., Amiri, F., Ahmad, N. B., Balasundram, S. K., & Soom, M. A. M. (2013). *Agriculture land suitability evaluator (alse): a decision and planning support tool for tropical and subtropical crops*. Computers and Electronics in Agriculture, 93, 98–110. <https://doi.org/10.1016/j.compag.2013.02.003>
11. Esri, Bauer, M.; Falloon, P.; Betts, R. (2010) *Climate impacts on European agriculture and water management in the context of adaptation and mitigation – the importance of and integrated approach*. Science of The Total Environment. 408(23), 5667–5687. DOI: <https://doi.org/10.1016/j.scitotenv.2009.05.002>.
12. Gao, J., & Liu, Y. (2010). *Determination of land degradation causes in tongyu county, northeast china via land cover change detection*. International Journal of Applied Earth Observations and Geoinformation, 12(1), 9–16. <https://doi.org/10.1016/j.jag.2009.08.003>
13. Gómez, C., White, J.C., Wulder, M.A. (2016) Optical remotely sensed time series data for land cover classification: A review. ISPRS Journal of Photogrammetry and Remote Sensing, 116, 55–72. DOI: <https://doi.org/10.1016/j.isprsjprs.2016.03.008>.
14. Goodess, C.; D. Jacob, M.; Déqué, J.; Gutiérrez, R; Huth, E.; Kendon, G.; Leckebusch, P.; Lorenz and V. Pavan, (2009). *Downscaling methods, data and tools for input to impacts assessments*. In: ENSEMBLES: Climate Change and its Impacts: Summary of Research and Results from the ENSEMBLES Project [van der Linden, P. and J.F.B. Mitchell (eds.)]. Met Office Hadley Centre, Exeter, UK, pp. 59-78.
15. Google. (2020). [Map Coordinates for Crăciunelu de Jos, Romania]. Retrieved 18/05/2020 from <https://www.google.com.au/maps/place/46%C2%B010'17.4%22N+23%C2%05'10.0%22E/@46.1682039,23.8332136,16z/data=!4m5!3m4!1s0x0:0x0!8m2!3d46.1715!4d23.8361?hl=en>.
16. Gries, T.;& Redlin, M. (2019). *Human-induced climate change: the impact of land-use change*. Theoretical and Applied Climatology, 135(3-4), 1031–1044. <https://doi.org/10.1007/s00704-018-2422-8>.
17. HemaLatha, M.; Varadarajan, S. & Pandian, Durai. (2019). *Feature enhancement of multispectral images using vegetation, water, and soil indices image fusion*. In Proceedings of the International Conference on ISMAC in Computational Vision and Bio-Engineering 2018, (pp. 329–337). DOI: https://doi.org/10.1007/978-3-030-00665-5_34.
18. Herold, M.; Mayaux, P.; Woodcock, C.; Baccini, A.; Schmullius, C. (2008). *Some challenges in global land cover mapping: An assessment of agreement and accuracy in existing 1 km datasets*. Remote Sensing of Environment, 112, 2538–2556. DOI: <https://doi.org/10.1016/j.rse.2007.11.013>.
19. Huete, A. R. (2004). Remote Sensing For Environmental Monitoring. In Brusseau, M. L, Environmental Monitoring and Characterisation, (pp 183-206). Tucson. Arizona: Elsevier inc. <https://doi.org/10.1016/B978-0-12-064477-3.X5000-0>.

20. Jackson, T.; Chen, D.; Cosh, M.; Li, F.; Anderson, M.; Walthall, C.; Doriaswamy P. & Hunt R. (2004). Vegetation water content mapping using Landsat data derived normalized difference water index for corn and soybeans. *Remote Sensing of Environment*. 94(4), 475–482. DOI: <https://doi.org/10.1016/j.rse.2003.10.021>
21. Jin, S.; Sader, S. A. (2005). *Comparison of time series tasseled cap wetness and the normalized difference moisture index in detecting forest disturbances*. *Remote Sensing of Environment*. 94(3), 364–372. DOI: <https://doi.org/10.1016/j.rse.2004.10.012>.
22. Kjellström, E.; G. Nikulin, U.; Hansson, G.; Strandberg, and A. Ullerstig, (2011). *21st century changes in the European climate: uncertainties derived from an ensemble of regional climate model simulations*. *Tellus A*, 63A(1), 24–40, doi: 10.1111/j.1600-0870.2010.00475.x
23. Le, H. T.; Rochelle-Newall, E.; Ribolzi, O.; Janeau, J. L.; Huon, S.; Latschack, K. & Pommier, T. (2020). *Land use strongly influences soil organic carbon and bacterial community export in runoff in tropical uplands*. *Land Degradation & Development*, 31(1), 118–132. <https://doi.org/10.1002/ldr.3433>,
24. Mărculeț, I. & Mărculeț G C. (2017). *Crăciunelu de Jos (județul Alba) denumiri geografice locale I*. *Pangeea*, 124–130, 124–130. <https://doi.org/10.29302/Pangeea17.20>.
25. McCarthy, M. J.; Colna, K. E.; El-Mezayen, M. M.; Laureano-Rosario, A. E.; Méndez-Lázaro, P.; Otis, D. B.; ... Muller-Karger, F. E. (2017). *Satellite remote sensing for coastal management: a review of successful applications*. *Environmental Management -New York-*, 60(2), 323–339.
26. Moon, T.; Ahlstrøm, A.; Goelzer, H. et al. *Rising Oceans Guaranteed: Arctic Land Ice Loss and Sea Level Rise*. *Curr Clim Change Rep* 4, 211–222 (2018). <https://doi.org/10.1007/s40641-018-0107-0>
27. National Institute of Statistics. (2017). Romania Regiuni Boundaries 2017. [feature service]. Retrieved from: <https://www.arcgis.com/home/item.html?id=c95580efef5848d1bd41682cb9f1d17b>
28. Natura 2000, (2019). [ROSCI0382, *Râul Târnava Mare între Copșa Mică și Mihalț*, Standard Data, Standar data form]. Retrieved from <http://natura2000.eea.europa.eu/Natura2000/SDF.aspx?site=ROSCI0382&release=10>.
28. Nelson, G. C.; Valin, H.; Sands, R. D.; Havlik, P.; Ahammad, H.; Deryng, D., ... Willenbockel, D. (2014). *Climate change effects on agriculture: economic responses to biophysical shocks. (special feature: economic sciences: agricultural sciences)*. *Proceedings of the National Academy of Sciences of the United States*, 111(9), 3274.
29. Parmentier, B.; Eastman, J.R. (2014). *Land transitions from multivariate time series: Using seasonal trend analysis and segmentation to detect land-cover changes*. *International Journal of Remote Sensing*. 35(2), 671–692. DOI: <https://doi.org/10.1080/01431161.2013.871595>.
30. Rhman, S.; Mesev, V. (2019). *Change Vector Analysis, Tasseled Cap, and NDVI-NDMI for Measuring Land Use/Cover Changes Caused by a Sudden Short-Term Severe Drought: 2011 Texas Event*. *Remote Sens*. 11(19), 2217. DOI: <https://doi.org/10.3390/rs11192217>.
31. Richards, J. A. (2014). *Remote sensing digital image analysis: an introduction (5., th ed. 2013)*. Springer Berlin.
32. Sexton, J.O.; Urban, D.L.; Donohue, M.J.; Song, C. (2013). *Long-term land cover dynamics by multi-temporal classification across the Landsat-5 record*. *Remote Sensing of Environment*. 128, 246–258. DOI: <https://doi.org/10.1016/j.rse.2012.10.010>.
33. Sima, M.; Popovici, E.; Bălțeanu, D.; Micu, D.; Kucsicsa, G.; Dragotă, C.; Grigorescu, I. (2015). *A farmer-based analysis of climate change adaptation options of agriculture*

- in the Bărăgan Plain, Romania*. Earth Perspectives. 2(5). DOI: <https://doi.org/10.1186/s40322-015-0031-6>.
34. Thornton, L. E.; Pearce, J. R.; & Kavanagh, A. M. (2011). *Using geographic information systems (GIS) to assess the role of the built environment in influencing obesity: a glossary*. International Journal of Behavioral Nutrition and Physical Activity, 8(1), 71–71. <https://doi.org/10.1186/1479-5868-8-71>
 35. Trenberth, K. (2011). *Changes in Precipitation with Climate Change*. Climate Change Research. Climate Research. 47. 123-138. DOI: 10.3354/cr00953.
 36. Trenberth, K. E. (2018). *Climate change caused by human activities is happening and it already has major consequences*. Journal of Energy & Natural Resources Law, 36(4), 463-481. <http://dx.doi.org.ezproxy.ecu.edu.au/10.1080/02646811.2018.1450895>.
 37. Turner, B. L. II; Lambin, E. F. & Reenberg, A. (2007). *The emergence of land change science for global environmental change and sustainability*. Proceedings of the National Academy of Sciences of the United State of America. 104(52), 20666–20671. DOI: <https://doi.org/10.1073/pnas.0704119104>.
 38. Turnock, D.; Vasile, C. S.; et al., (2020). *Romania*. Encyclopædia Britannica. Encyclopædia Britannica, inc. Retrieved from <https://www.britannica.com/place/Romania/Agriculture-forestry-and-fishing>.
 39. Vogel, M. M.; Zscheischler, J.; Wartenburger, R.; Dee, D. & Seneviratne, S. I. (2019). *Concurrent 2018 hot extremes across Northern Hemisphere due to human induced climate change*. Earth's Future, 7, 692– 703. <https://doi.org/10.1029/2019EF001189>.
 40. Wechsler, S.; Hyowon, B. & Li, L. (2019). *The Pervasive Challenge of Error and Uncertainty in Geospatial Data: Volume Eight*. Advanced Computing and Systems for Security, 315-332. DOI: 10.1007/978-3-030-04750-4_16.
 41. Williams, H.; Baartman, J.; McLelland, S.; Murphy, B.; Parsons, D. & van der Ploeg, M. (2019). *Investigating the role of sediment type, rainfall event sequence and vegetation cover on surface water flow and erosion patterns using a physical model*. In Geophysical Research Abstracts (21).
 42. World Bank Group; Climate Change Knowledge Portal [web]. (2020). *Romania. Climate data > Historical*. Accessed 02 June 2020 from: <https://climateknowledgeportal.worldbank.org/country/romania/climate-data-historical>.
 43. Yang, W.; Wang, Y.; He, C.; Xingyan, Tan, X.; & Han, Z. (2019). *Soil Water Content and Temperature Dynamics under Grassland Degradation: A Multi-Depth Continuous Measurement from the Agricultural Pastoral Ecotone in Northwest China*. Sustainability, 11(15), 1-14. DOI: 10.3390/su11154188.